

Origins of the fastest stars from merger-disruption of He-CO white dwarfs

Hila Glanz^{1,*,+}, Hagai B. Perets^{1,*,+}, Aakash Bhat^{2,3}, and Ruediger Pakmor⁴

*glanz@campus.technion.ac.il; hperets@physics.technion.ac.il

+these authors contributed equally to this work

¹Technion - Israel Institute of Technology, Haifa, 3200002, Israel

²Institut für Physik und Astronomie, Universität Potsdam, Karl-Liebknecht-Str. 24/25, 14476 Potsdam-Golm, Germany

³Dr. Karl-Remeis Observatory, Sternwartstr.7, 96049 Bamberg, Germany

⁴Max-Planck-Institut für Astrophysik, Karl-Schwarzschild-Str. 1, D-85748, Garching, Germany

ABSTRACT

Hypervelocity white dwarfs (HVWDs) are stellar remnants moving at speeds exceeding the Milky Way's escape velocity^{1–6}. The origins of the fastest HVWDs are enigmatic, with proposed formation scenarios facing challenges explaining both their extreme velocities and observed properties^{7,8}. Here we report a three-dimensional hydrodynamic simulation of a merger between two hybrid helium-carbon-oxygen white dwarfs (HeCO WDs with masses of 0.68 and 0.62 M_{\odot}). We find that the merger leads to a partial disruption of the secondary WD, coupled with a double-detonation explosion of the primary WD. This launches the remnant core of the secondary WD at a speed of 2000 km s^{-1} , consistent with observed HVWDs. The low mass of the ejected remnant and its heating from the primary WD's ejecta explain the observed luminosities and temperatures of hot HVWDs, which are otherwise difficult to reconcile with previous models. This discovery establishes a new formation channel for HVWDs and points to a previously unrecognized pathway for producing peculiar Type Ia supernovae and faint explosive transients.

Hypervelocity white dwarfs (HVWDs^{1,2,4,6}) are enigmatic objects, hurtling through our galaxy at speeds exceeding the Milky Way's escape velocity ($> 500 \text{ km s}^{-1}$; ⁹). Their existence challenges our understanding of stellar evolution and the dynamics of close binary systems. While most white dwarfs exhibit velocities typical of the Galactic disk or halo, HVWDs possess extreme speeds, implying a violent ejection mechanism. The advent of high-precision astrometry from the Gaia mission^{10,11} has led to the identification of seven HVWD candidates with velocities exceeding 1000 km/s ^{4,6}, further deepening the mystery surrounding their origin (lower velocity HVWDs were suggested to be produced from partial deflagration supernovae of WDs and later also identified; see^{1,2,6} and references therein). Of these, two of the first identified HVWDs (D6-2 and D6-3) have very low measured radial velocities (RVs), possibly inconsistent with the far higher measured tangential velocities, casting doubt on their identification as HVWDs and/or their measured velocities^{4,12,13}, while the other five have large radial velocities consistent with typical $\sim 2000 \text{ km s}^{-1}$ (see table in the supplementary information; SI). Older WDs might also have non-negligible peculiar velocities of up to a few hundred km s^{-1} suggesting a larger uncertainty in ejection velocity. In particular, in-going (towards the direction of the Galactic disk) HVWDs could not have originated from the disk, suggesting large ages and peculiar velocities for their progenitors at the time of ejection. D6-2 and J0927 are in-going HVWDs, which might suggest that the inferred extreme ejection velocity of J0927 (the highest velocity inferred; 2519^{+2716}_{-147}) could be lower, more in par with other HVWDs, and potentially closer to $\sim 2000 \text{ km s}^{-1}$, but conversely, could also be higher.

A leading hypothesis for the formation of such HVWDs involves the "dynamically driven double-degenerate double-detonation" (D6) scenario^{14–17} (based on earlier double detonation scenarios not involving two WDs^{18,19}). In this model, a close binary system consisting of two white dwarfs (one typically massive $> 0.85 M_{\odot}$) undergoes a gravitational wave inspiral. As the primary white dwarf accretes a small amount of Helium from its companion, a Helium detonation is triggered in the accreted and any low-mass pre-existing Helium shell, leading to a second, Carbon-detonation in the core and a Type Ia supernova explosion. The companion white dwarf, no longer gravitationally bound, is flung outward at high speed.

Nevertheless, the D6 scenario faces difficulties in explaining both the extreme HVWD velocities ($> 2000 \text{ km s}^{-1}$) and the observed properties of these objects. Recent studies^{7,8} have shown that detonation of a massive WD primary scenario as envisioned in the D6 scenario does not produce the high temperatures and inflated radii on observable timescales in some HVWDs, particularly for those with the highest velocities, for which the D6 scenario requires high mass HVWDs ($> 1 M_{\odot}$ ^{20,21}). Moreover, the predicted rate of HVWD formation from D6 events, if it were the main channel for the origin of type Ia SNe, appears to be significantly higher than the observed rate^{4,12}, and HVWDs were not found close to secure type Ia supernova

$M_{b,\text{Tot}}$ [M_{\odot}]	$M_{b,\text{He}}$ [M_{\odot}]	$M_{b,\text{IGE}}$ [M_{\odot}]	$M_{b,\text{IME}}$ [M_{\odot}]	Kick Velocity [km s^{-1}]	Angular Momentum [$\text{g cm}^2 \text{s}^{-1}$]
0.49	$3.1 \cdot 10^{-3}$	$3 \cdot 10^{-3}$	$1 \cdot 10^{-2}$	2061	2.48×10^{50}

Table 1. Final properties of the remnant (bound mass), where M_b stands for bound mass, the third column is the total mass of He in the remnant, the fourth column is the total mass of the elements we consider as an iron group (Scandium to Nickel), and the fifth is the total bound mass of the intermediate elements (Fluorine to Calcium). Bound material is calculated by finding all mass with a positive energy, including the internal energy. The velocity refers to the velocity of the highest central density region of the remnant. The last column shows the total angular momentum in the remnant.

remnants^{12,22}. More recent studies suggested that companions might also explode^{23–25}, which could potentially resolve the rates and supernova remnant issue, without significantly affecting the SN observations. However, in this case, no HVWD would form at all, requiring an alternative origin, like the one suggested here.

Here, we present a novel scenario for the origin of HVWDs based on a three-dimensional hydrodynamical simulation of a merger between two hybrid helium-carbon-oxygen white dwarfs (HeCO WDs). This simulation reveals a previously unexplored pathway for HVWD formation, distinct from the standard D6 model. We find that the merger of two HeCO WDs (0.68 and $0.62 M_{\odot}$) can lead to a partial tidal disruption of the lower-mass white dwarf (i.e. the secondary or companion), coupled with a double-detonation explosion of the primary. This process launches the remnant *low-mass* hot core of the disrupted white dwarf at hypervelocity speeds, which can remain inflated and hot for long timescales, consistent with observations. Thereby, our findings provide a compelling explanation for the origin of the fastest HVWDs and offer new insights into the diversity of explosive stellar phenomena.

We model the merger using 3D hydrodynamical simulation using the `AREPO` code²⁶ (see Methods). Figure 1 illustrates the key stages of the merger and explosion (A full movie showing the merger can be found in the SI, as well as a figure with more detailed snapshots; 2.2). As the secondary WD approaches the primary, it is tidally deformed and begins to transfer mass. This mass transfer eventually triggers a helium detonation on the surface of the primary WD. In the D6 scenario the high temperature and density conditions on the massive primary lead to early Helium detonation, occurring while the secondary is still intact, and after minimal accretion from the companion. However, in the low-mass HeCO cases shown here, a Helium detonation occurs only after the secondary has already begun to be significantly disrupted. In particular, a significant mass of Helium has already been transferred from the secondary to the primary, allowing for stronger, more energetic Helium detonation. The Helium detonation propagates around the primary, converging on the opposite side and driving a shock wave into the core. This shock wave initiates a secondary detonation in the carbon-oxygen core, leading to a supernova explosion, leaving the secondary unbound and ejected at a higher velocity. The very close approach and partial disruption allow for higher orbital (and eventually ejection) velocities and stronger heating of the companion.

Although the secondary WD is partially disrupted during the merger (stripped of $0.13 M_{\odot}$, and transferred $0.013 M_{\odot}$ to the primary), its core remains intact, when the Carbon-Oxygen detonation ensues. This core, tidally and debris-impact-heated and now unbound, is ejected following the supernova explosion at a velocity of 2061 km s^{-1} . The properties of the ejected remnant are summarized in Table 1. The remnant has a mass of $0.492 M_{\odot}$, including a small amount of helium ($0.003 M_{\odot}$) and traces of heavier elements synthesized during the explosion. Due to the strong tidal interaction during the merger, the ejected HVWD is expected to be rapidly rotating. The initial rotation velocity should be comparable to the ejection velocity. However, as the remnant expands and cools, its rotation velocity decreases due to angular momentum conservation. At the final snapshot of our simulation, the HVWD has a total angular momentum of $2.48 \times 10^{50} \text{ g cm}^2 \text{ s}^{-1}$; during its long-term evolution, the WD expands and its rotational velocity is expected to be significantly lower. For the currently inferred radius of $\sim 0.05 R_{\odot}$ for some of the HVWDs we would expect a rotation velocity of $\sim 770 \text{ km s}^{-1}$.

The supernova explosion resulting from the double detonation releases $1.13 \times 10^{51} \text{ erg}$ of nuclear energy (Table 2). The explosion ejects a total of $0.82 M_{\odot}$ of material, including $0.1 M_{\odot}$ of iron-group elements, of which $0.072 M_{\odot}$ in radioactive ^{56}Ni , and $0.42 M_{\odot}$ of intermediate-mass elements. Interestingly, the Helium shell burning and detonation prior to the CO detonation already produces a few $0.01 M_{\odot}$ of both radioactive ^{56}Ni , as well as faster decaying radioactive elements ^{48}Cr and ^{52}Fe which could affect the early light-curve, and typically not expected in normal type Ia SNe (see the radioactive elements production evolution in time in Fig. 2).

Table 1 summarizes the SN explosion properties. Given the low ^{56}Ni produced, the Helium burning products in the outer shells, and the relatively small amount of ejecta the SN is likely to be faint and peculiar. The mass and ^{56}Ni might be consistent with 91bg-like SNe, however such SNe are only observed in old environments in early-type galaxies²⁷. In addition, since the primary also had a large orbital velocity at the time of the explosion, SNe-producing HVWDs should have a large center of mass velocities. This could potentially be identified as a shift in velocity measurement of nebular spectra taken long after the explosion of such peculiar faint SN. The supernova remnant (SNR) of such SNe, if identified, should also have such a shift. In

Total Nuclear Energy [erg]	$M_{u,1}$ [M_{\odot}]	$M_{u,2}$ [M_{\odot}]	$M_{u,Tot}$ [M_{\odot}]	$M_{u,IGE}$ [M_{\odot}]	$M_{u,IME}$ [M_{\odot}]	SN CoM Velocity [km s^{-1}]
$1.126 \cdot 10^{51}$	0.68	0.14	0.82	0.1	0.42	1187

Table 2. Final properties of the supernova, where M_u stands for the total unbound mass, 1 stands for the ejected mass from the primary, and 2 for the secondary. IGE are Iron group elements (Scandium to Nickel), and IME are Intermediate elements (Fluorine to Calcium). SN velocity is the unbound mass’s center of mass velocity (CoM).

particular, if paired with an identified HVWD, it should have a velocity in counter direction to that of the HVWD. We find the SNR center of mass velocity in our simulation to be 1187 km s^{-1} .

Following the simulation we record the remnant properties (densities, compositions, temperature) found in the simulation, and then follow its long-term evolution, following the same approach as ref.⁷, by mapping the properties into 1D and then using the MESA stellar evolution code²⁸ (see Methods). Figure 3 shows the long-term evolution of the ejected HVWD in the Hertzsprung-Russell diagram (HR diagram). The remnant is initially hot and luminous, and experiences some super-Eddington mass-loss, but then cools and fades over time as it expands and releases its thermal energy. The low mass of the remnant contributes to its inflated state and prolonged cooling time.

The observed physical properties of several HVWD candidates are also plotted in Figure 3, taken from⁶, besides for J0927²⁹. The radius and temperature of our simulated remnant align well with the observed values, particularly for the HVWD J0546 and J1332, and to a lesser extent with J0927 (consistent within 2-sigma uncertainty, or 1σ , if ref.⁶ inferred temperature is adapted), but see further discussion on the properties J1332 in the SI, section 2.4. This suggests that our proposed formation scenario can explain the observed properties of the more reliable and highest-velocity HVWDs. That being said, D6-1 and J1235 do show consistent reliable high radial velocities but are not directly explained by our specific simulation. Nevertheless, given the large phase space of HeCO WD mergers, it is possible that more consistent models can be found with more/less massive HeCOs configurations (see also discussion on velocities in the SI, section 2.3).

Our 3D hydrodynamical simulation has revealed a new channel for the formation of HVWDs through the merger of two hybrid HeCO white dwarfs. This scenario differs significantly from the previously proposed D6 model, which involves the detonation of a *massive* CO white dwarf, following very little mass transfer, leaving the companion intact. In our simulation, the merger of two lower-mass HeCO WDs leads to a partial tidal disruption of the secondary WD and a double-detonation explosion of the low-mass primary. The close approach of the binary down to the point of partial tidal disruption allows for the larger velocity of the companion, even though the primary is relatively low-mass. Hence, this leads to the ejection of the remnant core of the secondary as an HVWD with a velocity exceeding 2000 km s^{-1} .

This novel channel offers several advantages in explaining the observed properties of HVWDs. First, it naturally produces the high ejection velocities observed for some HVWDs, which are difficult to achieve in the D6 scenario without invoking massive progenitor WDs, which are rare. Second, the low mass of the ejected remnant and its heating from the primary WD’s ejecta explain the observed luminosities and inflated radii of HVWDs, which can not be reconciled with the D6 model for HVWDs with such velocities.

Our findings have broader implications for our understanding of stellar evolution and explosive transients. They highlight the potential importance of HeCO WDs in producing a variety of thermonuclear events. The merger of HeCO WDs may lead to peculiar Type Ia supernovae with fainter luminosities and potentially distinct observational signatures compared to standard SNe Ia. Further studies are needed to characterize the detailed properties of these explosions and their potential contribution to the observed diversity of SNe Ia.

The discovery of HVWDs was initially hailed as a smoking-gun signature of the D6 scenario and its potential role in producing the majority of SNe Ia. However, our results suggest that HVWDs may originate from a wider range of progenitor systems and explosion mechanisms. This casts doubt on the D6 scenario as the dominant channel for SNe Ia and emphasizes the need to explore alternative pathways.

The current study is limited by the computational cost of 3D hydrodynamical simulations, which restricts the exploration of wider parameter space of HeCO WD mergers. Future studies with larger parameter surveys will help to constrain the range of HVWD properties and the rates of these events. Nevertheless, our findings clearly demonstrate the viability of HeCO WD mergers as a source of HVWDs and open up new avenues for research into the explosive fates of binary white dwarf systems (see also^{24,30,31} for other explosive transients involving HeCO WDs). Moreover, analytic estimates (see SI; section 2.3) suggest that it is likely that the phase space of merging double HeCO WDs could produce HVWDs of a wider range of velocities and masses beyond the specific point derived from the fully modeled case shown here. It could naturally explain (and predict) a wider range of velocities in the range $2000 \pm 300 \text{ km s}^{-1}$ expected for HVWDs from the partial HeCO tidal-disruption channel. Indeed, the inferred velocities (within the $1 - \sigma$ uncertainties) of all besides D6-2 (which is the least reliable given its very low radial velocity) of the HVWDs reside in this range. In fact, these might explain the preference for this velocity range.

In summary, we have demonstrated that the merger of two HeCO WDs can produce HVWDs with properties consistent with observations, both in terms of ejection velocities, ages, and physical properties. This novel channel provides a compelling explanation for the origin of the fastest HVWDs and sheds new light on the diversity of explosive transients in the Universe.

1 Methods

We investigate the formation of HVWDs through the merger of two hybrid helium-carbon-oxygen (HeCO) white dwarfs using a three-dimensional magnetohydrodynamical simulation. This is the first study to explore this scenario, in particular, in 3D, allowing us to capture the complex dynamics of the merger process and the subsequent ejection of the HVWD.

1.1 HeCO White Dwarfs

HeCO white dwarfs are a class of stellar remnants characterized by a helium-rich outer layer surrounding a carbon-oxygen core. Their formation is linked to binary star interactions, where processes like Roche lobe overflow and common envelope evolution lead to the accumulation of helium on the white dwarf^{24,32,33}. These hybrid WDs can have masses and compositions that fall between those of typical helium WDs and carbon-oxygen WDs, making their merger outcomes particularly interesting.

More specifically, we investigate the fate of a double degenerate binary system consisting of a primary Helium-rich HeCO WD, with the total mass of $0.69 M_{\odot}$ made of a CO core of $0.59 M_{\odot}$ and a massive helium shell of $0.1 M_{\odot}$ (see details in²⁴), and a secondary hybrid HeCO WD with total mass of $0.62 M_{\odot}$ made of a CO core of $0.58 M_{\odot}$ and a massive helium shell of $0.038 M_{\odot}$ (following³⁴). Note, that the much higher He shell for this hybrid is attained through a somewhat different evolution than that described in³⁵, as explored in²⁴.

For the density profile and composition of the $0.62 M_{\odot}$ WD, we use a similar method as in³⁶, where we generate the 1D profile in hydrostatic equilibrium, with $0.0365 M_{\odot}$ He shell, following the results of³³.

1.2 Hydrodynamical Simulation

We model the merger of two HeCO white dwarfs using the moving-mesh hydrodynamics code `Arepo`^{37–40}. This code provides a self-gravitating, adaptive mesh framework for simulating astrophysical phenomena, incorporating a Helmholtz equation of state for degenerate matter and a 55 isotope nuclear reaction network to capture the thermonuclear processes involved in the merger. A detailed description of WD merger simulations in `Arepo` can be found in²⁴, and our models closely follow similar approaches and modeling. We run our simulation with a cell mass resolution of 9×10^{26} g, a minimum cell volume of $\sim 10^{19}$ cm³, $\sim 3.510^6$ cells, in a total box size of 10^{12} cm to incorporate the explosion and the expansion of the remnant.

1.2.1 Initial Conditions

The initial conditions for our simulation are derived from 1D stellar evolution models. These models provide the density, temperature, and composition profiles for both the primary and secondary HeCO white dwarfs. The specific parameters of our simulated binary system are:

Primary WD: Mass = $0.69 M_{\odot}$, CO core = $0.59 M_{\odot}$, He shell = $0.1 M_{\odot}$ as modelled in²⁴ using `MESA`^{28,41,42}, and mapped to 3D. **Secondary WD:** Mass = $0.62 M_{\odot}$, CO core = $0.58 M_{\odot}$, He shell = $0.038 M_{\odot}$, where the composition is based on `MESA` models in³³. This model was generated synthetically in the same method as in³⁶.

The 3D white dwarf models are initialized in `Arepo`, relaxed to ensure stability, and then placed in a binary configuration within a large simulation domain. The initial separation of the binary is chosen to be wide enough to minimize initial tidal forces, 5.1×10^4 km, and the corresponding orbital period was 177.5s.

1.2.2 Inspiral and Merger

We simulate the inspiral of the binary system, initially accelerating it by artificially removing angular momentum to mimic the effect of gravitational wave emission. This artificial inspiral is halted just before the secondary WD enters the Roche radius of the primary and mass transfer becomes dynamically significant (see²⁴ for a similar approach and further details). The binary separation at this point was 2.37×10^4 km, with an orbital period of 8.7s.

We then follow the fully realistic evolution of the merger. As the secondary WD approaches the primary, it is tidally deformed and disrupted (~ 100 s after the end of the accelerated inspiral stage). The dynamical mass transfer of helium from the secondary triggers a helium detonation on the surface of the primary. This detonation propagates around the primary, leading to a secondary detonation in the carbon-oxygen core and a supernova explosion. The partially disrupted secondary WD, still containing its core, is ejected at high velocity by the force of the explosion. These stages are presented in Figure 4 in the SI, while some are also in Figure 1 of the main part. A full movie of the simulation can be found in the SI.

1.3 Evolution of the Bound Remnant HVWD

To model the long-term evolution of the runaway WD we follow a similar approach as in⁷. We map the output of the simulation (~ 300 s after the explosion) to the 1D stellar evolution software `MESA`. This procedure has been applied before for `Athena++`

Name	v_r [km s ⁻¹]	v_{tot} [km s ⁻¹]	$v_{ejection}$ [km s ⁻¹]	T_{eff} [K]	R [R_\odot]	d [kpc]	z [kpc]	t_{disk} [Myr]
D6-1	1200±40	2045 ⁺²⁵¹ ₋₁₉₀	2254 ⁺²⁴⁸ ₋₁₉₉	7000	0.23 ^{+0.04} _{-0.03}	1.91 ^{+0.2} _{-0.2}	-0.57 ^{+0.07} _{-0.06}	0.63 ^{+0.04} _{-0.04}
D6-2	80±10	1151 ⁺⁵⁹ ₋₅₅	1051 ⁺⁶² ₋₅₂	7000	0.15 ^{+0.01} _{-0.01}	0.84 ^{+0.05} _{-0.04}	-0.27 ^{+0.01} _{-0.02}	-0.72 ^{+0.01} _{-0.01}
D6-3	-20±80	2248 ⁺³⁴⁰ ₋₃₂₄	2393 ⁺³⁷⁷ ₋₃₉₆	7000	0.17 ^{+0.02} _{-0.02}	2.26 ^{+0.34} _{-0.35}	0.93 ^{+0.14} _{-0.14}	2.24 ^{+0.21} _{-0.17}
J1235-3752	-1694±10	2670 ⁺³³⁹ ₋₂₅₀	2471 ⁺³⁵¹ ₋₂₅₆	21000	0.104 ^{+0.026} _{-0.030}	4.53 ^{+2.17} _{-1.82}	1.73 ^{+0.42} _{-0.50}	1.87 ^{+0.86} _{-0.25}
J0927-6335	-2285±20	2753 ⁺²⁷¹ ₋₁₄₈	2519 ⁺²⁷¹ ₋₁₄₇	60000	0.052 ^{+0.025} _{-0.020}	4.07 ^{+1.01} _{-0.70}	-0.70 ^{+0.27} _{-0.35}	-1.32 ^{+0.42} _{-0.42}
J0546+0836	1200±20	1699 ⁺⁶⁶⁰ ₋₃₉₀	1864 ⁺⁶⁸² ₋₄₁₆	95000	0.051 ^{+0.029} _{-0.021}	4.02 ^{+2.29} _{-1.67}	-0.69 ^{+0.29} _{-0.40}	0.61 ^{+0.08} _{-0.08}
J1332-3541	1090±50	1464 ⁺⁷⁰⁷ ₋₃₃₁	1619 ⁺⁷⁰⁷ ₋₃₂₀	70000	0.017 ^{+0.013} _{-0.007}	1.63 ^{+1.19} _{-0.68}	0.74 ^{+0.53} _{-0.30}	0.64 ^{+0.13} _{-0.14}

Table 3. Kinematic and physical properties of suspected D6 hypervelocity white dwarfs, including radial velocity, total velocity, ejection velocity, effective temperature, radius, distance, height above the Galactic plane, and flight time back to the Galactic disk.

simulations of helium subdwarfs²⁰ and more recently of helium white dwarfs⁸, as well as *Arepo* simulations of massive white dwarfs⁷. Here, we follow the procedure outlined in reference⁷. The 3D profiles of the runaway WD (taken at the last snapshot, which is 10-20 times dynamical timescales after the explosion, allowing sufficient time for the WD to adjust) are averaged to give a 1D profile with temperature, density, and mass fraction information. A 22 isotope network `approx_21_plusco56` is used to model the nuclear reactions during this evolution and includes the isotopes ¹H, ^{3,4}He, ¹²C, ¹⁴N, ¹⁶O, ²⁰Ne, ²⁴Mg, ²⁸Si, ³²S, ³⁶Ar, ⁴⁰Ca, ⁴⁴Ti, ^{48,56}Cr, ^{52,54,56}Fe, ⁵⁶Co, and ⁵⁶Ni. It therefore includes the most important reactions of nickel decay and α capture on carbon. We relax a white dwarf to our output profiles of composition and entropy, as outlined in⁷, and we get rid of almost all of the outer layers where ⁵⁶Ni dominates the atmosphere to such an extent that the material will become unbound on short timescales (but longer than the hydrodynamical simulation). This cut is chosen again to be the mass coordinate where the energy due to ⁵⁶Ni decay is twice the gravitational binding energy of the star. This results in a final mass of 0.482 M_\odot , with only 0.005 M_\odot cut-off. Once relaxed the white dwarf is allowed to evolve for a maximum time of 100 Myr.

2 Supplementary Information

This supplementary information provides additional details and supporting material for the main text.

2.1 The properties of the hypervelocity WDs

Table 3 summarizes the physical and kinematic properties of the seven fastest hypervelocity WDs, from tables 2 and 3 in ref.⁶ (kinematics and radii) and from Refs.^{4,29,43,44} for the temperatures and radii.

2.2 Detailed evolution of the merger: Movie and snapshots

A movie visualizing the merger of the two HeCO white dwarfs and the subsequent ejection of the HVWD is available online¹. The movie shows the tidal disruption of the secondary WD, the double-detonation explosion of the primary, and the high-velocity ejection of the remnant core.

In addition, we provide more detailed snapshots of the evolution in Fig. 4

2.3 Analytic Estimate of Ejection Velocities

The ejection velocity of the HVWD can be estimated analytically by considering the Keplerian velocity of the binary system at the time of the explosion. Assuming that the explosion occurs near the tidal radius, the ejection velocity of the secondary is given by:

$$v_{ej} \approx \frac{M_1}{M_{tot}} \sqrt{\frac{GM_{tot}}{R_{tid}}}, \quad (1)$$

where G is the gravitational constant, M_{tot} is the total mass of the binary system, and R_{tid} is the tidal radius. The Tidal radius can be approximated as:

$$R_{tid} \approx R_1 \left(\frac{2M_1}{M_2} \right)^{1/3}, \quad (2)$$

¹<https://tinyurl.com/dd2hyperv>

Where R_1 is the radius of the primary WD and M_1 and M_2 are the masses of the primary and secondary WDs, respectively. The radii of the WDs are calculated using the mass-radius relation formulation by ref.⁴⁵.

Figure 5 shows the expected ejection velocities for a range of binary WD progenitors, calculated using such an analytic estimate. The measured ejection velocity in our simulation matches the analytic prediction well. Nevertheless, this simplified estimate should be taken with a grain of salt, given that the final stages of the tidal evolution and deformation before the SN explosion affect the orbit and the structure of the WDs, and even some of the companion mass is stripped; hence these should only be considered as order of magnitude expectations as to bracket the range of possible ejection velocities in the double HeCO WD merger scenario.

2.4 The properties of HVWD J1332

Given that in both the D6 scenario and our model, the outer layers of the ejected HVWD are stripped, it is unlikely that such a WD would have a hydrogen atmosphere. Therefore, we do not adapt the properties of the HVWD inferred by²⁹ for J1332 using a hydrogen-rich atmosphere, but the ones assuming a Helium outer atmosphere (hotter and puffier). Nevertheless, for completeness, in Figure 6 we show the HR diagram, radius, and temperature models, and their comparison with observations of J1332 if the hydrogen-rich model of²⁹ is taken at face value. In that case, the HR position is only consistent within $2 - \sigma$ and the inferred radius is no longer consistent with our simulation results. One should note that in that case, J1332 could be consistent with a model of a far more massive CO HVWD, as discussed in⁷.

2.5 Population Synthesis Considerations

Population synthesis studies suggest that mergers involving hybrid WDs are not rare among double WD mergers, with as much as 25% of WD mergers including at least one hybrid WD^{30,31}. The mergers of double HeCO WDs represent only a fraction of these, with a smaller fraction likely producing the specific conditions required for the partial disruption and double-detonation explosion observed in our simulation. If such explosions are a significant source of HVWDs, their relatively low occurrence rate could explain the paucity of HVWDs compared to the rate of normal Type Ia SNe.

2.6 Observational Signatures

The peculiar Type Ia SNe produced by the HeCO WD merger scenario are expected to have fainter luminosities and different observational signatures compared to standard SNe Ia. These differences arise from the lower mass of the exploding WD and the distinct composition of the ejecta. Further studies are needed to characterize the detailed observational properties of these explosions and their potential contribution to the observed diversity of SNe Ia. These will be explored in future studies.

3 Software and third party data repository citations

We make use of the following codes: `Arepo`^{37,38,40,46}, `MESA`^{28,41,42,47}, `Matplotlib`⁴⁸, `NumPy`⁴⁹, and `SciPy`⁵⁰. MESA inlists will be made available through the MESA community on Zenodo.

References

1. Jordan, I., George C., Perets, H. B., Fisher, R. T. & van Rossum, D. R. Failed-detonation Supernovae: Subluminous Low-velocity Ia Supernovae and their Kicked Remnant White Dwarfs with Iron-rich Cores. *Astrophys. J. Lett.* **761**, L23, DOI: [10.1088/2041-8205/761/2/L23](https://doi.org/10.1088/2041-8205/761/2/L23) (2012). [1208.5069](https://arxiv.org/abs/1208.5069).
2. Vennes, S. *et al.* An unusual white dwarf star may be a surviving remnant of a subluminous Type Ia supernova. *Science* **357**, 680–683, DOI: [10.1126/science.aam8378](https://doi.org/10.1126/science.aam8378) (2017). [1708.05568](https://arxiv.org/abs/1708.05568).
3. Raddi, R. *et al.* Further Insight on the Hypervelocity White Dwarf, LP 40-365 (GD 492): A Nearby Emissary from a Single-degenerate Type Ia Supernova. *Astrophys. J.* **858**, 3, DOI: [10.3847/1538-4357/aab899](https://doi.org/10.3847/1538-4357/aab899) (2018). [1803.07564](https://arxiv.org/abs/1803.07564).
4. Shen, K. J. *et al.* Three Hypervelocity White Dwarfs in Gaia DR2: Evidence for Dynamically Driven Double-degenerate Double-detonation Type Ia Supernovae. *Astrophys. J.* **865**, 15, DOI: [10.3847/1538-4357/aad55b](https://doi.org/10.3847/1538-4357/aad55b) (2018). [1804.11163](https://arxiv.org/abs/1804.11163).
5. Raddi, R. *et al.* Partly burnt runaway stellar remnants from peculiar thermonuclear supernovae. *Mon. Not. R. Astron. Soc.* **489**, 1489–1508, DOI: [10.1093/mnras/stz1618](https://doi.org/10.1093/mnras/stz1618) (2019). [1902.05061](https://arxiv.org/abs/1902.05061).
6. El-Badry, K. *et al.* The fastest stars in the Galaxy. *The Open J. Astrophys.* **6**, 28, DOI: [10.21105/astro.2306.03914](https://doi.org/10.21105/astro.2306.03914) (2023). [2306.03914](https://arxiv.org/abs/2306.03914).
7. Bhat, A. *et al.* Supernova Shocks Cannot Explain the Inflated State of Hypervelocity Runaways from White Dwarf Binaries. *arXiv e-prints* arXiv:2407.03424, DOI: [10.48550/arXiv.2407.03424](https://doi.org/10.48550/arXiv.2407.03424) (2024). [2407.03424](https://arxiv.org/abs/2407.03424).

8. Wong, T. L. S., White, C. J. & Bildsten, L. Shocking and Mass Loss of Compact Donor Stars in Type Ia Supernovae. *Astron. Astrophys. J.* **973**, 65, DOI: [10.3847/1538-4357/ad6a11](https://doi.org/10.3847/1538-4357/ad6a11) (2024). [2408.00125](https://arxiv.org/abs/2408.00125).
9. Brown, W. R. Hypervelocity Stars. *Annu. Rev. Astron. Astrophys.* **53**, 15–49, DOI: [10.1146/annurev-astro-082214-122230](https://doi.org/10.1146/annurev-astro-082214-122230) (2015).
10. Gaia Collaboration *et al.* Gaia Data Release 2. Summary of the contents and survey properties. *Astron. Astrophys.* **616**, A1, DOI: [10.1051/0004-6361/201833051](https://doi.org/10.1051/0004-6361/201833051) (2018). [1804.09365](https://arxiv.org/abs/1804.09365).
11. Gaia Collaboration *et al.* Gaia Data Release 3. Summary of the content and survey properties. *Astron. Astrophys.* **674**, A1, DOI: [10.1051/0004-6361/202243940](https://doi.org/10.1051/0004-6361/202243940) (2023). [2208.00211](https://arxiv.org/abs/2208.00211).
12. Igoshev, A. P., Perets, H. & Hallakoun, N. Hyper-runaway and hypervelocity white dwarf candidates in Gaia Data Release 3: Possible remnants from Ia/Iax supernova explosions or dynamical encounters. *Mon. Not. R. Astron. Soc.* **518**, 6223–6237, DOI: [10.1093/mnras/stac3488](https://doi.org/10.1093/mnras/stac3488) (2023). [2209.09915](https://arxiv.org/abs/2209.09915).
13. Scholz, R. D. Hypervelocity star candidates from Gaia DR2 and DR3 proper motions and parallaxes. *Astron. Astrophys.* **685**, A162, DOI: [10.1051/0004-6361/202348430](https://doi.org/10.1051/0004-6361/202348430) (2024). [2402.10714](https://arxiv.org/abs/2402.10714).
14. Guillochon, J., Dan, M., Ramirez-Ruiz, E. & Rosswog, S. Surface Detonations in Double Degenerate Binary Systems Triggered by Accretion Stream Instabilities. *Astrophys. J. Lett.* **709**, L64–L69, DOI: [10.1088/2041-8205/709/1/L64](https://doi.org/10.1088/2041-8205/709/1/L64) (2010). [0911.0416](https://arxiv.org/abs/0911.0416).
15. Pakmor, R., Kromer, M., Taubenberger, S. & Springel, V. Helium-ignited Violent Mergers as a Unified Model for Normal and Rapidly Declining Type Ia Supernovae. *Astrophys. J. Lett.* **770**, L8, DOI: [10.1088/2041-8205/770/1/L8](https://doi.org/10.1088/2041-8205/770/1/L8) (2013). [1302.2913](https://arxiv.org/abs/1302.2913).
16. Sato, Y. *et al.* A Systematic Study of Carbon-Oxygen White Dwarf Mergers: Mass Combinations for Type Ia Supernovae. *Astrophys. J.* **807**, 105, DOI: [10.1088/0004-637X/807/1/105](https://doi.org/10.1088/0004-637X/807/1/105) (2015). [1505.01646](https://arxiv.org/abs/1505.01646).
17. Shen, K. J. *et al.* Three Hypervelocity White Dwarfs in Gaia DR2: Evidence for Dynamically Driven Double-degenerate Double-detonation Type Ia Supernovae. *Astrophys. J.* **865**, 15, DOI: [10.3847/1538-4357/aad55b](https://doi.org/10.3847/1538-4357/aad55b) (2018). [1804.11163](https://arxiv.org/abs/1804.11163).
18. Iben, I., Jr. & Tutukov, A. V. On the evolution of close binaries with components of initial mass between 3 solar masses and 12 solar masses. *Astrophys. J. Suppl. Ser.* **58**, 661–710, DOI: [10.1086/191054](https://doi.org/10.1086/191054) (1985).
19. Iben, J., Icko, Nomoto, K., Tornambe, A. & Tutukov, A. V. On Interacting Helium Star–White Dwarf Pairs as Supernova Precursors. *Astrophys. J.* **317**, 717, DOI: [10.1086/165318](https://doi.org/10.1086/165318) (1987).
20. Bauer, E. B., White, C. J. & Bildsten, L. Remnants of Subdwarf Helium Donor Stars Ejected from Close Binaries with Thermonuclear Supernovae. *Astrophys. J.* **887**, 68, DOI: [10.3847/1538-4357/ab4ea4](https://doi.org/10.3847/1538-4357/ab4ea4) (2019). [1906.08941](https://arxiv.org/abs/1906.08941).
21. Bauer, E. B., Chandra, V., Shen, K. J. & Hermes, J. J. Masses of White Dwarf Binary Companions to Type Ia Supernovae Measured from Runaway Velocities. *Astrophys. J. Lett.* **923**, L34, DOI: [10.3847/2041-8213/ac432d](https://doi.org/10.3847/2041-8213/ac432d) (2021). [2112.03189](https://arxiv.org/abs/2112.03189).
22. Shields, J. V. *et al.* No Surviving SN Ia Companion in SNR 0509-67.5: Stellar Population Characterization and Comparison to Models. *Astrophys. J. Lett.* **950**, L10, DOI: [10.3847/2041-8213/acd6a0](https://doi.org/10.3847/2041-8213/acd6a0) (2023). [2305.03750](https://arxiv.org/abs/2305.03750).
23. Tanikawa, A., Nomoto, K., Nakasato, N. & Maeda, K. Double-detonation Models for Type Ia Supernovae: Trigger of Detonation in Companion White Dwarfs and Signatures of Companions’ Stripped-off Materials. *Astrophys. J.* **885**, 103, DOI: [10.3847/1538-4357/ab46b6](https://doi.org/10.3847/1538-4357/ab46b6) (2019). [1909.09770](https://arxiv.org/abs/1909.09770).
24. Pakmor, R., Zenati, Y., Perets, H. B. & Toonen, S. Thermonuclear explosion of a massive hybrid HeCO white dwarf triggered by a He detonation on a companion. *Mon. Not. R. Astron. Soc.* **503**, 4734–4747, DOI: [10.1093/mnras/stab686](https://doi.org/10.1093/mnras/stab686) (2021). [2103.06277](https://arxiv.org/abs/2103.06277).
25. Pakmor, R. *et al.* On the fate of the secondary white dwarf in double-degenerate double-detonation Type Ia supernovae. *Mon. Not. R. Astron. Soc.* **517**, 5260–5271, DOI: [10.1093/mnras/stac3107](https://doi.org/10.1093/mnras/stac3107) (2022). [2203.14990](https://arxiv.org/abs/2203.14990).
26. Springel, V. E pur si muove: Galilean-invariant cosmological hydrodynamical simulations on a moving mesh. *Mon. Not. R. Astron. Soc.* **401**, 791–851, DOI: [10.1111/j.1365-2966.2009.15715.x](https://doi.org/10.1111/j.1365-2966.2009.15715.x) (2010). [0901.4107](https://arxiv.org/abs/0901.4107).
27. Perets, H. B. *et al.* A faint type of supernova from a white dwarf with a helium-rich companion. *Nature* **465**, 322–325, DOI: [10.1038/nature09056](https://doi.org/10.1038/nature09056) (2010). [0906.2003](https://arxiv.org/abs/0906.2003).
28. Paxton, B. *et al.* Modules for Experiments in Stellar Astrophysics (MESA). *Astrophys. J. Suppl. Ser.* **192**, 3, DOI: [10.1088/0067-0049/192/1/3](https://doi.org/10.1088/0067-0049/192/1/3) (2011). [1009.1622](https://arxiv.org/abs/1009.1622).
29. Werner, K., El-Badry, K., Gänsicke, B. T. & Shen, K. J. Ultraviolet spectroscopy of the supernova Ia hypervelocity runaway white dwarf J0927-6335. *Astron. Astrophys.* **689**, L6, DOI: [10.1051/0004-6361/202451635](https://doi.org/10.1051/0004-6361/202451635) (2024). [2408.08397](https://arxiv.org/abs/2408.08397).

30. Perets, H. B., Zenati, Y., Toonen, S. & Bobrick, A. Normal type Ia supernovae from disruptions of hybrid He-CO white-dwarfs by CO white-dwarfs. *arXiv e-prints* arXiv:1910.07532, DOI: [10.48550/arXiv.1910.07532](https://doi.org/10.48550/arXiv.1910.07532) (2019). [1910.07532](https://arxiv.org/abs/1910.07532).
31. Zenati, Y. *et al.* The Origins of Calcium-rich Supernovae From Disruptions of CO White Dwarfs by Hybrid He-CO White Dwarfs. *Astrophys. J.* **944**, 22, DOI: [10.3847/1538-4357/acaf65](https://doi.org/10.3847/1538-4357/acaf65) (2023). [2207.13110](https://arxiv.org/abs/2207.13110).
32. Iben, J., I. & Tutukov, A. V. On the evolution of close binaries with components of initial mass between 3 M and 12 M. *Astrophys. J. Suppl. Ser.* **58**, 661–710, DOI: [10.1086/191054](https://doi.org/10.1086/191054) (1985).
33. Zenati, Y., Toonen, S. & Perets, H. B. Formation and evolution of hybrid He–CO white dwarfs and their properties. *Mon. Notices Royal Astron. Soc.* **482**, 1135–1142, DOI: [10.1093/mnras/sty2723](https://doi.org/10.1093/mnras/sty2723) (2018). <http://oup.prod.sis.lan/mnras/article-pdf/482/1/1135/26205282/sty2723.pdf>.
34. Zenati, Y., Perets, H. B. & Toonen, S. Neutron star-white dwarf mergers: early evolution, physical properties, and outcomes. *Mon. Not. R. Astron. Soc.* **486**, 1805–1813, DOI: [10.1093/mnras/stz316](https://doi.org/10.1093/mnras/stz316) (2019). [1807.09777](https://arxiv.org/abs/1807.09777).
35. Zenati, Y., Toonen, S. & Perets, H. B. Formation and evolution of hybrid He-CO white dwarfs and their properties. *Mon. Not. R. Astron. Soc.* **482**, 1135–1142, DOI: [10.1093/mnras/sty2723](https://doi.org/10.1093/mnras/sty2723) (2019). [1803.04444](https://arxiv.org/abs/1803.04444).
36. Pakmor, R. *et al.* On the fate of the secondary white dwarf in double-degenerate double-detonation Type Ia supernovae. *Mon. Not. R. Astron. Soc.* **517**, 5260–5271, DOI: [10.1093/mnras/stac3107](https://doi.org/10.1093/mnras/stac3107) (2022). [2203.14990](https://arxiv.org/abs/2203.14990).
37. Springel, V. E pur si muove: Galilean-invariant cosmological hydrodynamical simulations on a moving mesh. *Mon. Not. R. Astron. Soc.* **401**, 791–851, DOI: [10.1111/j.1365-2966.2009.15715.x](https://doi.org/10.1111/j.1365-2966.2009.15715.x) (2010). [0901.4107](https://arxiv.org/abs/0901.4107).
38. Pakmor, R., Bauer, A. & Springel, V. Magnetohydrodynamics on an unstructured moving grid. *Mon. Not. R. Astron. Soc.* **418**, 1392–1401, DOI: [10.1111/j.1365-2966.2011.19591.x](https://doi.org/10.1111/j.1365-2966.2011.19591.x) (2011). [1108.1792](https://arxiv.org/abs/1108.1792).
39. Zhu, C., Pakmor, R., van Kerkwijk, M. H. & Chang, P. Magnetized Moving Mesh Merger of a Carbon-Oxygen White Dwarf Binary. *Astrophys. J. Lett.* **806**, L1, DOI: [10.1088/2041-8205/806/1/L1](https://doi.org/10.1088/2041-8205/806/1/L1) (2015). [1504.01732](https://arxiv.org/abs/1504.01732).
40. Weinberger, R., Springel, V. & Pakmor, R. The AREPO Public Code Release. *Astrophys. J. Suppl. Ser.* **248**, 32, DOI: [10.3847/1538-4365/ab908c](https://doi.org/10.3847/1538-4365/ab908c) (2020). [1909.04667](https://arxiv.org/abs/1909.04667).
41. Paxton, B. *et al.* Modules for Experiments in Stellar Astrophysics (MESA): Planets, Oscillations, Rotation, and Massive Stars. *Astrophys. J. Suppl. Ser.* **208**, 4, DOI: [10.1088/0067-0049/208/1/4](https://doi.org/10.1088/0067-0049/208/1/4) (2013). [1301.0319](https://arxiv.org/abs/1301.0319).
42. Paxton, B. *et al.* Modules for Experiments in Stellar Astrophysics (MESA): Pulsating Variable Stars, Rotation, Convective Boundaries, and Energy Conservation. *Astrophys. J. Suppl. Ser.* **243**, 10, DOI: [10.3847/1538-4365/ab2241](https://doi.org/10.3847/1538-4365/ab2241) (2019). [1903.01426](https://arxiv.org/abs/1903.01426).
43. Chandra, V. *et al.* The SN Ia runaway LP 398-9: detection of circumstellar material and surface rotation. *Mon. Not. R. Astron. Soc.* **512**, 6122–6133, DOI: [10.1093/mnras/stac883](https://doi.org/10.1093/mnras/stac883) (2022). [2110.06935](https://arxiv.org/abs/2110.06935).
44. Werner, K., Reindl, N., Rauch, T., El-Badry, K. & Bédard, A. The photospheres of the hottest fastest stars in the Galaxy. *Astron. Astrophys.* **682**, A42, DOI: [10.1051/0004-6361/202348286](https://doi.org/10.1051/0004-6361/202348286) (2024). [2311.13388](https://arxiv.org/abs/2311.13388).
45. Nauenberg, M. Analytic Approximations to the Mass-Radius Relation and Energy of Zero-Temperature Stars. *Astrophys. J.* **175**, 417, DOI: [10.1086/151568](https://doi.org/10.1086/151568) (1972).
46. Pakmor, R. *et al.* Improving the convergence properties of the moving-mesh code AREPO. *Mon. Not. R. Astron. Soc.* **455**, 1134–1143, DOI: [10.1093/mnras/stv2380](https://doi.org/10.1093/mnras/stv2380) (2016). [1503.00562](https://arxiv.org/abs/1503.00562).
47. Jermyn, A. S. *et al.* Modules for Experiments in Stellar Astrophysics (MESA): Time-dependent Convection, Energy Conservation, Automatic Differentiation, and Infrastructure. *Astrophys. J. Suppl. Ser.* **265**, 15, DOI: [10.3847/1538-4365/acae8d](https://doi.org/10.3847/1538-4365/acae8d) (2023). [2208.03651](https://arxiv.org/abs/2208.03651).
48. Hunter, J. D. Matplotlib: A 2d graphics environment. *Comput. Sci. & Eng.* **9**, 90–95, DOI: [10.1109/MCSE.2007.55](https://doi.org/10.1109/MCSE.2007.55) (2007).
49. Harris, C. R. *et al.* Array programming with NumPy. *Nature* **585**, 357–362, DOI: [10.1038/s41586-020-2649-2](https://doi.org/10.1038/s41586-020-2649-2) (2020).
50. Virtanen, P. *et al.* SciPy 1.0: Fundamental Algorithms for Scientific Computing in Python. *Nat. Methods* **17**, 261–272, DOI: [10.1038/s41592-019-0686-2](https://doi.org/10.1038/s41592-019-0686-2) (2020).

Acknowledgments

HBP acknowledges support for this project from the European Union’s Horizon 2020 research and innovation program under grant agreement No 865932-ERC-SNeX. HG acknowledges support for the project from the Council for Higher Education of Israel. A.B. was supported by the Deutsche Forschungsgemeinschaft (DFG) through grant GE2506/18-1 and by the Kavli Summer Program which took place at MPA in Garching in July 2023, and was supported by the Kavli Foundation. We would like to thank Evan Bauer and Robert Fisher for their valuable comments and discussions.

Author contributions statement

HG led the key research, ran the hydrodynamical simulations, and analyzed their results. HBP initiated and supervised the project, suggested the main ideas, analyzed the results, and wrote the main parts of the paper. AB made the long-term WD evolution modeling and analyzed them. RP assisted with running the hydrodynamical simulations. All authors contributed to writing the paper, making the figures, and reviewing the manuscript.

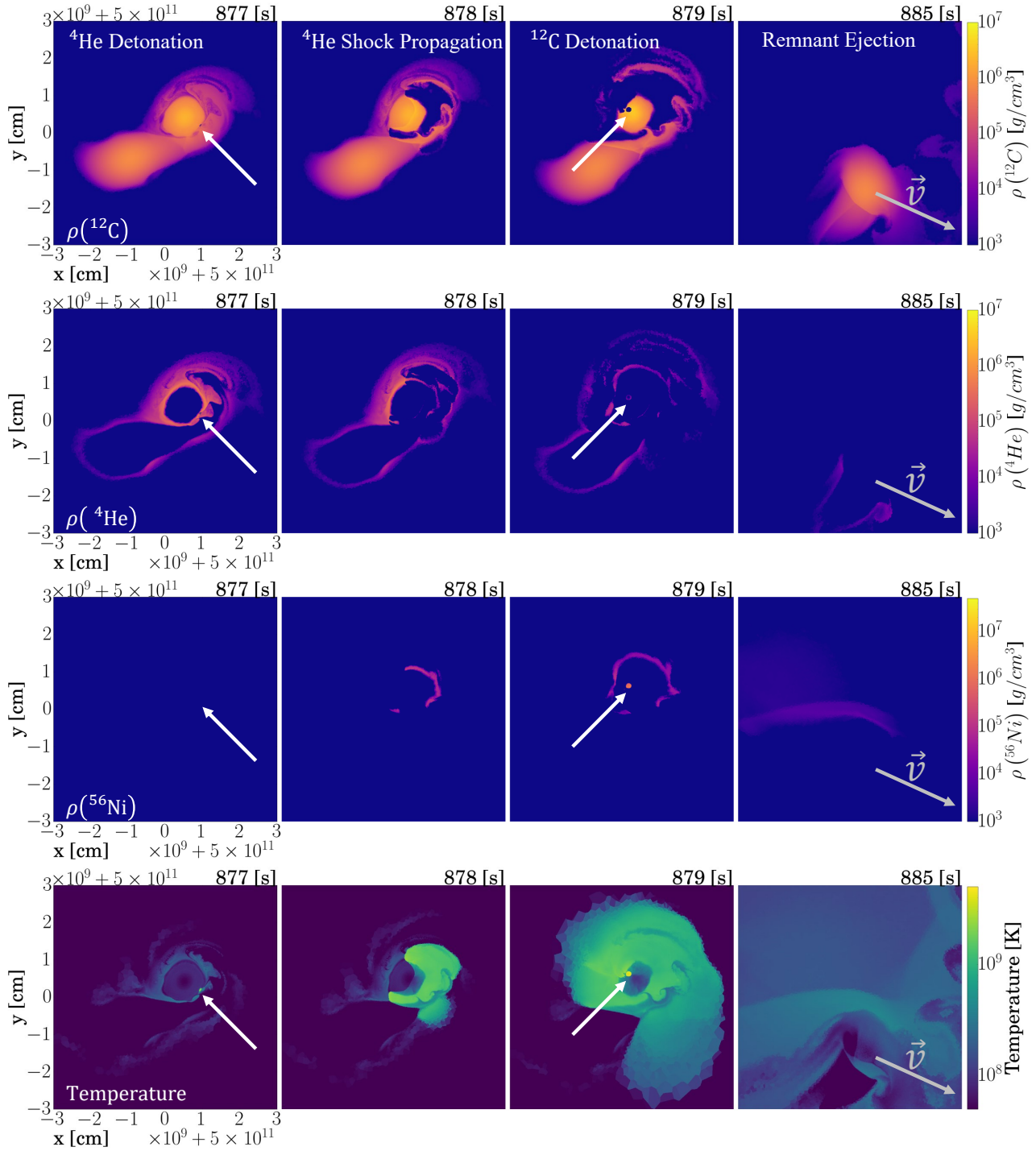


Figure 1. The panels show the time evolution from the time of the ignition of the helium detonation (left panels) to the time when the shock converges in the CO core of the primary WD (third from the left), and finally the ejected remnant in the right panels.

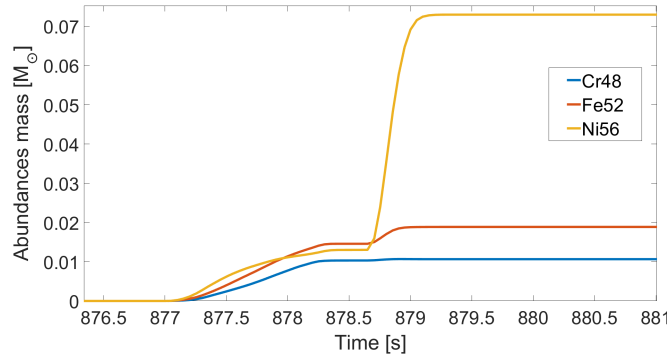


Figure 2. Production of radioactive elements throughout the merger. The early Helium burning and detonation already produces a significant amount of radioactive elements, with a few $0.01 M_{\odot}$ of radioactive ^{56}Ni , as well as faster decaying radioactive elements ^{48}Cr and ^{52}Fe produced at this stage. The bulk of the ^{56}Ni is produced by the CO detonation beginning at $t=878.8$ s.

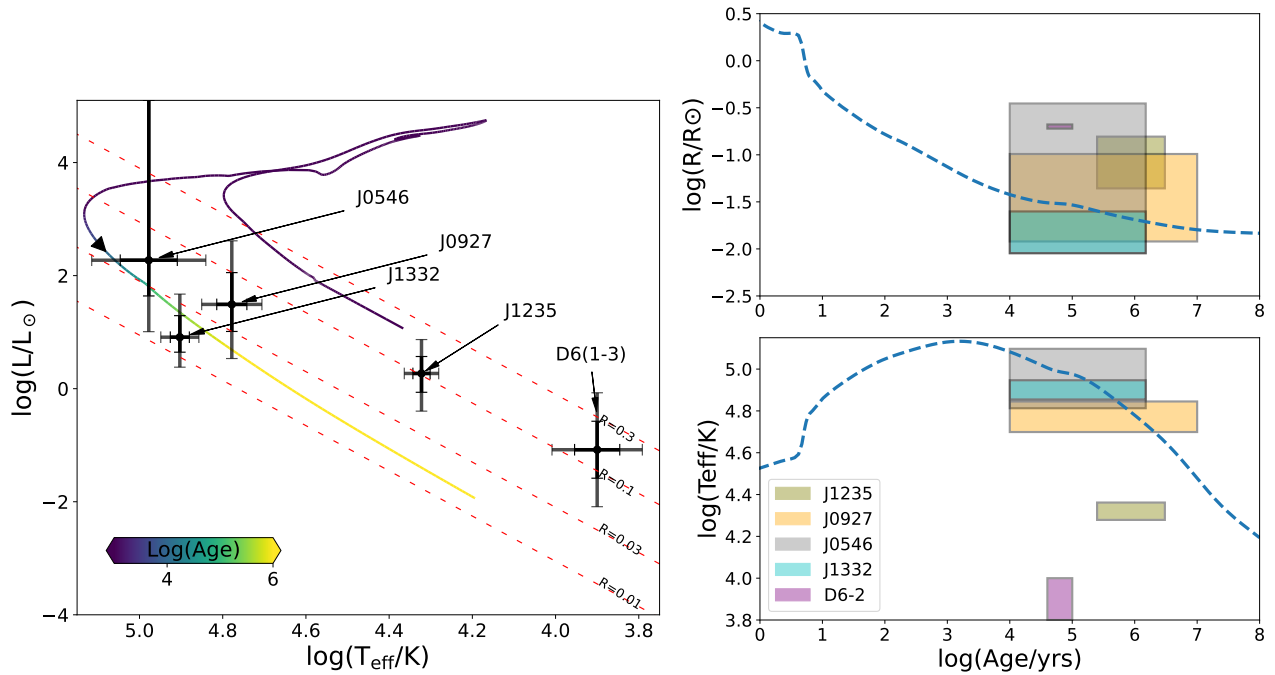


Figure 3. Left: The HR diagram for our model compared with the observed values. The error bars depict the 1 and 2σ uncertainties. The black arrow marks the point when the star is 10^4 years old. Right: The radius and temperature evolution of the model as a function of its age. In particular, the HVWDs J0546, J1332, and J0927 may be explained by our model, within the 1 -sigma (J0546, J1332) and 2σ (J0927; or 1σ too, if ref.⁶ inferred temperature is adapted) uncertainties, but see further discussion in the SI regarding J1332 [2.4](#)

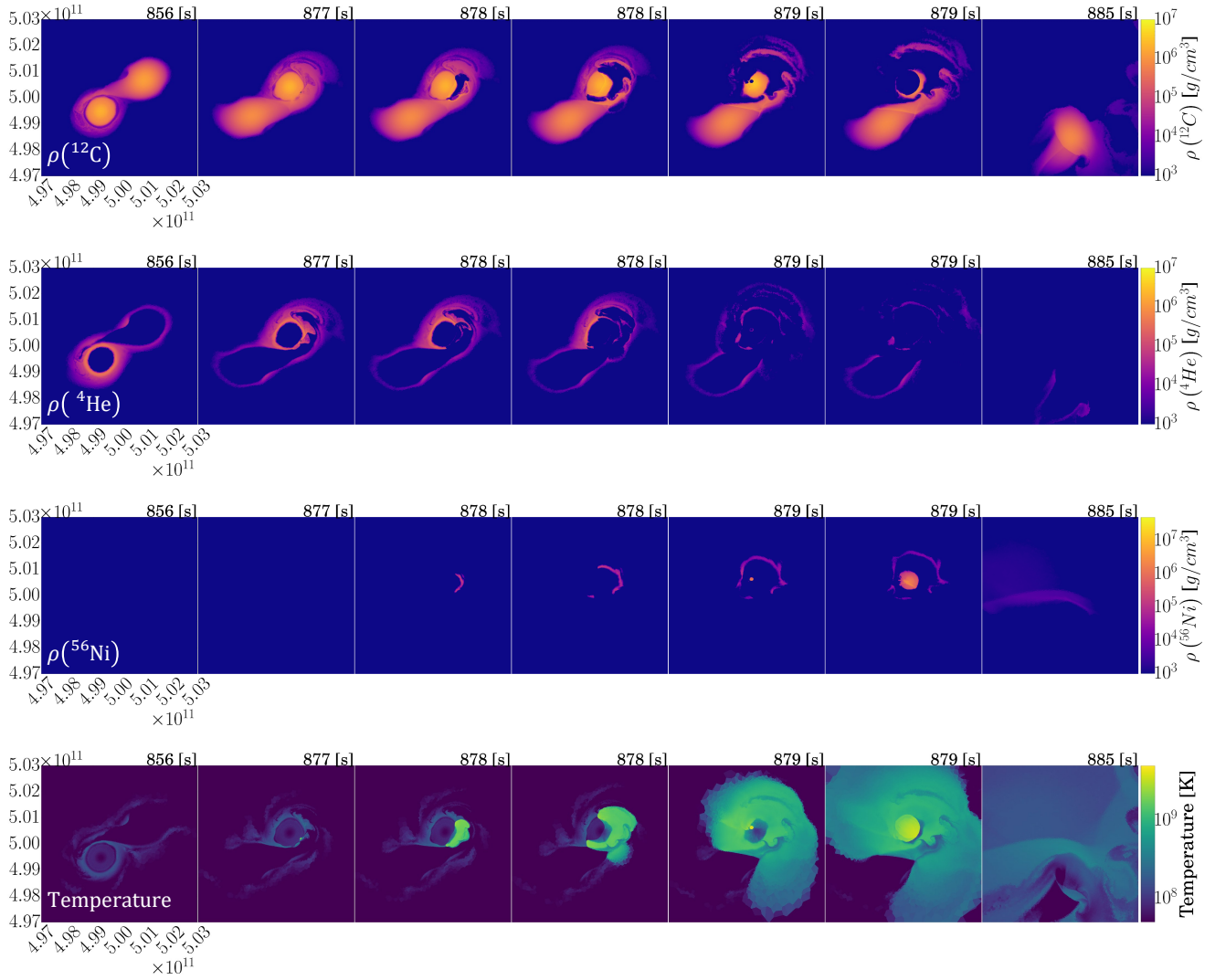


Figure 4. The panels show the time evolution from the time of the partial disruption of the secondary WD (left panels) to the time of the He detonation (second left) when the shock converges in the CO core of the primary WD (third from the left), and finally the ejected remnant in the right panels.

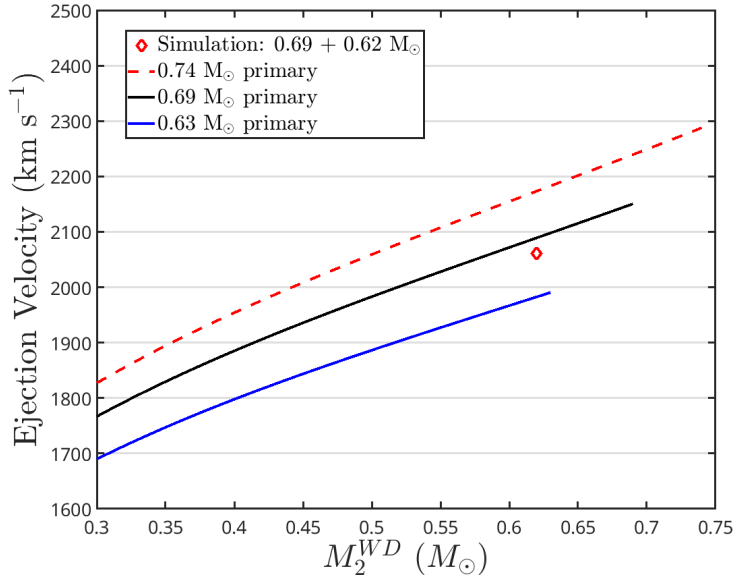


Figure 5. Expected ejection velocities of partially disrupted WDs from merging binary HeCO WD progenitors. Three primary masses are shown, corresponding to the upper mass expected for HeCO WDs ($0.74 M_{\odot}$); the simulated primary ($0.69 M_{\odot}$); and a lower mass primary expected to experience a double detonation ($0.63 M_{\odot}$; likely a lower limit). The measured ejection velocity in the simulation well matched the simple analytic estimate.

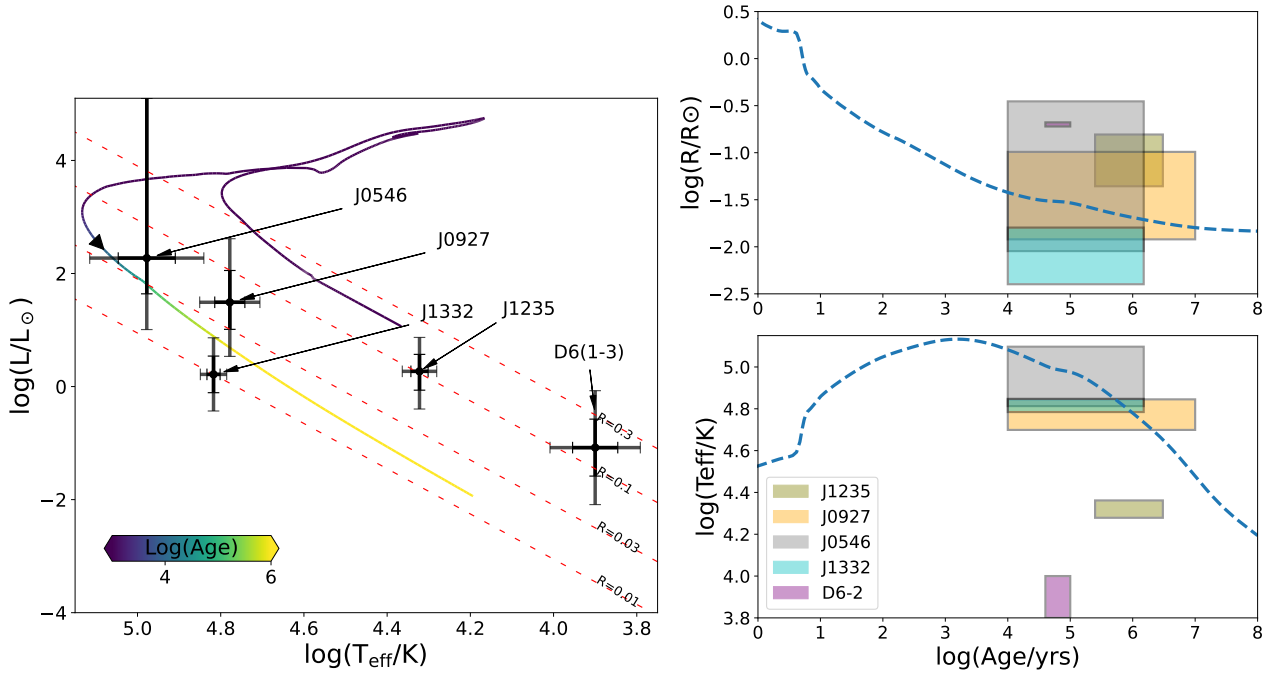


Figure 6. Left: The HR diagram for our model compared with the observed values, assuming a hydrogen-dominated atmosphere for J1332 based on ref.²⁹. The error bars depict the 1 and 2σ uncertainties. The black arrow marks the point when the star is 10^4 years old. Right: The radius and temperature evolution of the model as a function of its age. In particular, the HR positions of HVWDs J0546, J1332, and J0927 may be explained by our model, within the 1-sigma (J0546) and 2-sigma (J0927, J1332); as well as the temperatures of these WDs, while the radius of J1332 is inconsistent, if hydrogen atmosphere is assumed for J1332